Dual function of a secreted fungalysin metalloprotease in *Ustilago maydis*

Bilal Ökmen[1], Bastian Kemmerich[1], Daniel Hilbig[1], Raphael Wemhöner[1], Jörn Aschenbroich[2], Andreas Perrar[3], Pitter F. Huesgen[3], Kerstin Schipper[2], Gunther Doehlemann[1*]

1 *Botanical Institute and Cluster of Excellence on Plant Sciences (CEPLAS), University of Cologne, BioCenter, Zuelpicher Str. 47a, 50674 Cologne, Germany.*

2 *Institute for Microbiology, Heinrich Heine University, Universitätsstraße 1, 40225 Düsseldorf, Germany.*

3 *Central Institute for Engineering, Electronics and Analytics, ZEA-3, Forschungszentrum Jülich, Wilhelm-Johnen-Str., 52428 Jülich, Germany.*

[*]Address correspondence to:
Gunther Doehlemann
Tel: +49 221 470 1647
Email: g.doehlemann@uni-koeln.de

This is the peer reviewed author version of the following article as published online by the New Phytologist on 2018 Jun 19 and in print in New Phytol (2018) 220(1):249-261. The final version is published at https://doi.org/10.1111/nph.15265. This article may be used for non-commercial purposes in accordance with Wiley Terms and Conditions for Self-Archiving.

Key words: effector, chitinase, maize, metalloprotease, *Ustilago maydis*

Summary

- Fungalysins from several phytopathogenic fungi have been shown to be involved in cleavage of plant chitinases. While fungal chitinases are responsible for cell-wall remodeling during growth and morphogenesis, plant chitinases are important components of immunity. This study describes a dual function of the *Ustilago maydis* fungalysin UmFly1 in modulation of both plant and fungal chitinases.
- Genetic, biochemical and microscopic experiments were performed to elucidate the *in vitro* and *in planta* functions of *U. maydis* UmFly1.
- *U. maydis* Δ*umfly1* mutants show significantly reduced virulence, which coincides with reduced cleavage of the maize chitinase ZmChiA within its chitin-binding domain. Moreover, deletion of *umfly1* affected cell separation of haploid *U. maydis* sporidia. This phenotype is associated with posttranslational activation of the endogenous chitinase UmCts1. Genetic complementation of the Δ*umfly1* mutant with a homologous gene from closely related, but non-pathogenic yeast fully rescued the cell separation defect *in vitro* but it could not recover the Δ*umfly1* defect in virulence and cleavage of the maize chitinase.
- Here we report on the dual function of the secreted fungalysin UmFly1. We hypothesize that co-evolution of *U. maydis* with its host plant extended the endogenous function of UmFly1 towards the modulation of plant chitinase activity to promote infection.

Introduction

Chitinases are present in a wide range of organisms, including bacteria, archaea, fungi, plants and animals. They catalyze the hydrolysis of chitin, the main cell wall component of fungi, to its *N*-acetylglucosamine units. In fungi, chitinases play an important role in cell-wall remodeling during cell division (Kuranda & Robbins, 1991). In addition, they are also involved in nutritional chitin acquisition and competition with other fungi (Leake & Read 1990). The number of chitinase genes in fungi shows high variation, but they exclusively belong to the glycosyl hydrolase 18 (GH18) family (Langner & Gohre, 2016).

In plants, chitinases are pathogenesis-related (PR) proteins contributing to the plant defense against fungal infections. They are upregulated upon both biotic and abiotic stresses (Kasprzewska, 2003; Shoresh & Harman, 2008). Plant chitinase-mediated hydrolysis of fungal chitin contributes to two major plant defense responses: i) disassembly of the fungal cell wall, which leads to the inhibition of hyphal growth (Schlumbaum *et al.*, 1986); ii) and moreover, cleaved chitin fragments that are released from the fungal cell wall serve as elicitors for plant immune responses (Shibuya & Minami, 2001; Kaku *et al.*, 2006). According to the CAZy database, chitinases are classified into GH18 and GH19 families (Henrissat & Davies, 1997) (http://www.cazy.org/). While GH18 members are found in viruses, bacteria, fungi, plants and animals, GH19 family members are mostly present in plant species (Shoresh & Harman, 2008). In addition, based on their amino acid sequence similarity GH18 and GH19 are also grouped in different structural classes, including class III and V, and class I, II and IV, respectively (http://www.cazy.org/). The plant endochitinases of classes I, II and IV are considered to be PR3 proteins, while class III and class V members are considered to be PR8 and PR11 proteins, respectively (Kasprzewska, 2003). It has been reported that the maize genome encodes 31 putative chitinases including 27 endochitinases and four exochitinases (Shoresh & Harman, 2008). Class IV chitinases, such as maize ZmChiA and ZmChiB, are well characterized and were shown to inhibit the growth of several fungi on agar plates (Schlumbaum *et al.*, 1986; Huynh *et al.*, 1992).

During co-evolution between pathogenic fungi and their plant hosts, fungal pathogens have evolved diverse strategies to avoid or suppress chitinase-related defense mechanisms. For example, the causal agent of tomato leaf mold disease *Cladosporium fulvum* secretes the chitin binding protein Avr4, which shields the fungal cell wall and hereby protects it against plant

chitinase-mediated hydrolysis (van den Burg *et al.*, 2006; van Esse *et al.*, 2007). Another strategy is represented by a group of effector proteins containing LysM (Lysine motif) domains. An example is given again by *C. fulvum,* which secretes the chitin binding LysM protein Ecp6 (de Jonge *et al.*, 2010). Ecp6 efficiently binds and sequesters chitin fragments that are released from the fungal cell wall and hence, prevents the recognition of chitin fragments by pattern recognition receptors (PRRs) (de Jonge *et al.*, 2010). LysM effectors are widely distributed in the fungal kingdom (Bolton *et al.*, 2008) and some of them are functionally similar to Ecp6 (*Magnaporthe oryzae* and *Zymoseptoria tritici*) (Marshall *et al.*, 2011; Mentlak *et al.*, 2012). Furthermore, Vander *et al*., (1998) reported that when the degree of acetylation in chitosan is increased, it can induce more plant defense responses. This indicates that fungal chitin deacetylases may help plant pathogens to decrease their elicitor activity by deacetylation of chitin (El Gueddari *et al*., 2002; Duplessis *et al.*, 2011; Veneault-Fourrey *et al.*, 2014). Another group of phytopathogenic fungi copes differently with the detrimental effect of plant chitinases. Naumann *et al*. (2011, 2013) reported that various phytopathogenic *Fusarium* species secrete fungalysin proteins with a M36 metalloprotease domain to target and cleave class IV plant chitinases within a poly-glycine hinge domain in order to separate the chitin-binding domain (CBD) from the hydrolysis domain (Naumann *et al.*, 2011; Naumann & Wicklow, 2013). Since then, it has been reported that several other plant pathogenic filamentous ascomycetes, including *Alternaria brassicicola*, *Colletotrichum higginsianum*, *Verticillium longisoprum*, *V. dahlia*, and *Botrytis cinerea*, also have the ability to cleave plant class-IV chitinases (Naumann & Wicklow, 2013; Jashni *et al.*, 2015). Recently, Sanz-Martin *et al.*, (2016) showed that a fungalysin metalloprotease gene (*Cgfl*) in *Colletotrichum graminicola* is also involved in fungal virulence on maize, suggesting that chitinase-cleavage activity of fungalysin is required for full virulence. Moreover, it has been shown that inhibition of fungalysin in *Fusarium verticillioides* by using a wheat hevein-like peptide also inhibits the hyphal elongation, indicating that fungalysin plays a role in fungal development as well (Slavokhotova *et al*., 2014).

The biotrophic fungus *Ustilago maydis* belongs to the *Basidiomycota* and is the causative agent of corn smut disease (Kämper *et al.*, 2006). Upon maize penetration, *U. maydis* secretes hundreds of effector proteins to interfere with the plant immune machinery in various ways (e.g. by inhibition of defense-related cysteine proteases) in order to support its own growth and reproduction (Lo Presti *et al.*, 2015). During early stages (upon penetration) and later stages

(upon tumor formation) of infection, the transcripts of several classes of PR genes, including genes encoding maize chitinases, are elevated in *U. maydis* infected tissue (Doehlemann *et al.*, 2008). While effectors interfering with other core components of plant immunity have been identified (i.e. suppressors of the oxidative burst and apoplastic cysteine proteases) (Hemetsberger *et al.*, 2012; Mueller *et al.*, 2013), it remains unknown how *U. maydis* counteracts the activity of maize chitinases, because its genome does not encode Avr4- or Ecp6-like effectors. In the present study, we describe the fungalysin metalloprotease UmFly1 as a virulence factor of *U. maydis,* which is required for cleavage of the maize chitinase ZmChiA to remove the chitin binding domain from the GH19 domain. Independently of its virulence function, UmFly1 is also involved in cell separation of *U. maydis* sporidia where it regulates the processing and activation of an endogenous fungal chitinase. We suggest that this dual function of UmFly1 reflects the evolutionary adaptation of an endogenous protease to the plant infectious life style of *U. maydis.*

Materials and Methods

Growth condition for bacterial, fungal, and maize strains and virulence assay

Maize (*Zea mays* L. cv Early Golden Bantam) plants were grown in a temperature controlled greenhouse (14 hours:10 hours light:dark cycle, at 28:20°C with 40% humidity).

For virulence assays, *Ustilago maydis* strains were grown in $YEPS_{light}$ liquid medium at 28°C and 200 rpm to an OD_{600} of 0.6-0.8. Fungal and bacterial strains used in this study and their *g*rowth conditions are indicated in **Methods S1**. The *U. maydis* virulence assay was performed as described in the **Methods S1**.

Nucleic acids methods

Isolation of fungal genomic DNA, RNA and bacterial plasmids was performed as described in the **Methods S1**. Briefly, the isolation of genomic DNA of *U. maydis* was performed according to the protocol described by Schultz *et al*. (1990) (Schulz *et al.*, 1990) and total RNA was isolated from crushed leaf samples by using the TRIzol® extraction method (Invitrogen; Karlsruhe, Germany) according to the manufacturer's instructions. In addition, cDNA synthesis protocol and qRT-PCR assay were also indicated in the **Methods S1**. Results of at least three

biological qRT-PCR replicates were analyzed using the $2^{-\Delta Ct}$ method (Livak & Schmittgen, 2001). The primers used for qRT-PCR are listed in **Table S1**.

For plasmid construction, standard molecular biology methods were used according to molecular cloning laboratory manual of Sambrook *et al*. (1989) (Sambrook *et al.*, 1989). Detailed cloning procedures are depicted in the **Methods S1**.

Yeast Two-Hybrid assay

The adenine, histidine, leucine and tryptophan auxotroph *Saccharomyces cerevisiae* AH109 strain was used for Y2H system. A detailed description of the performed Yeast Two-Hybrid assays is provided in the **Methods S1**.

Heterologous protein production in *Pichia pastoris*

The *Pichia pastoris* KM71H-OCH gene expression system was used to produce N-terminally His-tagged UmFly1, N-terminally His and 3xHA tagged His-3xHA-ZmChiA and N-terminally His and C-terminally eGFP tagged His-Cts1-eGFP recombinant proteins. The *His-UmFly1*, *His-3xHA-ZmChiA* and *His-cts1-eGFP* were cloned into *pGAPZαA* vector (Invitrogen; Carlsbad, USA) under the control of a constitutive promotor with an α-factor signal peptide for secretion. Expression and purification of recombinant proteins were performed according to manufacturer's instructions (*pGAPZαA*, *B*, & *C Pichia pastoris* Expression Vectors, Invitrogen; Carlsbad, USA). Detailed expression procedure is described in the **Methods S1**.

Chitinase cleavage assay

The His-3xHA-ZmChiA and His-Cts1-eGFP cleavage assays were performed as described in the **Methods S1**.

Mass spectrometry for identification of cleavage sites

Details on ZmChiA and Cts1-eGFP sample preparation procedures, mass spectrometry data acquisition and data analysis are provided in the **Methods S1**.

Chitinase activity assays

After incubation of 300 µl ZmChiA (0.4 mg ml^{-1} in 10 mM NaAcetate buffer, pH 5.3) with 300 µl of SG200 and SG200Δumfly1 culture filtrate and $YEPS_{light}$ medium (concentrated) at 28°C for 12 hours, 600 µl of chitin-azur (5.6 mg ml^{-1} K-Phosphate buffer pH 6.0) (Sigma Aldrich,; Taufkirchen, Germany) was incubated with 300 µl of the reaction mix at 37°C overnight to check whether cleaved ZmChiA has less activity compared to the full length protein. The absorbance was measured at 560 nm. Cts1 activity assays were performed with 4-methylumbelliferyl-β-D-N,N',N''-triacetyl-chitotriose (Sigma Aldrich; Taufkirchen, Germany) (MUC) as described in Langner *et al.* (2015) (Langner *et al.*, 2015).

Microscopy and bioinformatics procedures

Staining for microscopy and bioinformatics procedures were described in the **Methods S1**.

Results

***Ustilago maydis UmFly1* is evolutionarily conserved in other fungi**

Homology based BLAST searches of the full length *Fusarium verticillioides* FvFly1 protein (Naumann *et al.*, 2011) in the *U. maydis* proteome revealed the presence of UMAG06098, which shares 37% amino acid (aa) identity with FvFly1. Hereafter, we will refer to the UMAG06098 protein as UmFly1 (encoded by the single copy gene *UMAG06098* (*umfly1*)). *In silico* analysis predicts that the 974 amino acids (aa) containing UmFly1 has a 36 aa N-terminal signal peptide, a fungalysin/thermolysin propeptide motif and a fungalysin M36 metalloprotease domain, which contains the characteristic HEXXH active site motif for Zn metalloproteases **(Fig. S1)**. Similarity analysis showed that the N-terminal part of UmFly1 has a low degree of similarity to FvFly1 (22.75%), whereas its C-terminal part is highly similar to FvFly1 (51.53%). A high level of conservation in the predicted catalytic M36 metalloprotease domain suggests that UmFly1 could also possess hydrolytic activity for plant chitinases **(Fig. S1)** (Li & Zhang, 2014; Sanz-Martin *et al.*, 2016). A phylogenetic analysis shows wide conservation of Fly1 homologs throughout the fungal kingdom including species with different life styles such as saprophytes, endophytes, as well as plant and animal pathogenic fungi **(Fig. S2)**. While in most cases *fly1* is a single copy gene, some fungal species including the plant pathogens *Verticillium dahliae* and *Microsporum canis* have multiple copies, indicating gene duplication events during evolution (Brouta *et al*., 2002; Li & Zhang, 2014).

Cleavage of ZmChiA by secreted UmFly1

To analyze the expression pattern of genes encoding maize chitinases during infection, quantitative real-time PCR (qRT-PCR) analysis was performed with total RNA isolated from maize leaves inoculated with the solopathogenic *U. maydis* strain SG200 (Kämper *et al.*, 2006) and from mock-treated leaves at 1, 2, 3, 6 and 9 days post infection (dpi). The qRT-PCR results revealed that the expression of *ZmChiA, B* and *C* was significantly up-regulated in *U. maydis*-infected leaves compared to mock controls (**Fig. 1a**). While *ZmChiA* and *ZmChiB* showed strong up-regulation at 1, 6 and 9 dpi, *ZmChiC* was significantly induced especially at 6 dpi (**Fig. 1a**). With respect to its high expression levels compared to *ZmChiB,* as well as the fact that ZmChiC does not contain a predicted chitin binding domain, the ZmChiA protein was selected for heterologous production in *P. pastoris*.

To test if *U. maydis* secretes enzymes that cleave ZmChiA, the supernatant of axenic *U. maydis* SG200 culture was incubated with purified ZmChiA protein at 28°C for 18 hours. As a negative control, ZmChiA was co-incubated with non-inoculated *U. maydis* growth medium ($YEPS_{light}$). Subsequent SDS-PAGE analysis showed that ZmChiA was cleaved after co-incubation with the *U. maydis* culture filtrate **(Fig. 1b)**. In addition to full length ZmChiA, three additional bands representing cleavage products with sizes between 26-35 kDa were observed **(Fig. 1b)**. In contrast, ZmChiA incubated with only $YEPS_{light}$ medium remained unprocessed **(Fig. 1b)**, suggesting the secretion of ZmChiA cleaving enzyme/s by *U. maydis*. To investigate whether UmFly1 is required for cleavage of ZmChiA, the *umfly1* gene was deleted by targeted gene replacement with a *hygromycin* resistance cassette to generate a SG200Δumfly1 mutant strain. For a subsequent ZmChiA cleavage assay, the culture filtrate was also prepared from SG200Δumfly1 strain, as it has been done for the *U. maydis* SG200 strain. No cleavage of ZmChiA was observed upon co-incubation with the culture filtrate of the SG200Δumfly1 strain (**Fig. 1c)**. To exclude that unspecific effects during gene replacement caused this effect, genetic complementation was performed by re-introducing the *umfly1* gene including its native promoter into the *ip*-locus of SG200Δumfly1 (Loubradou *et al.*, 2001). The resulting strain SG200Δumfly1-C showed ZmChiA cleavage indistinguishable from SG200, verifying that the ZmChiA cleavage was specifically dependent on the *umfly1* gene (**Fig. 1c)**. To test whether the cleavage of ZmChiA also requires the enzymatic activity of UmFly1, the predicted active site residues ^{729}HEYSH^{733} were replaced with ^{729}QQYSH^{733} by site directed mutagenesis and the

mutated *umfly1* gene was used for complementation of SG200Δumfly1 to generate the SG200Δumfly1-C_{mut} strain. The ZmChiA cleavage assay revealed no cleavage of ZmChiA by the SG200Δumfly1-C_{mut} strain, indicating that the enzymatic activity of UmFly1 is required for cleavage of ZmChiA (**Fig. 1c)**. Southern blot analysis was performed for all strains to confirm gene replacement, complementation and single integration events **(Fig. S3a-d)**.

To test whether UmFly1 directly interacts with ZmChiA, a yeast two-hybrid (Y2H) assay was performed. Proper expression of both BD-ZmChiA and AD-UmFly1 fusion proteins in yeast were verified by western blot analysis **(Fig. S4)**. No yeast growth was observed for empty vector controls with either *pGBKT7-ZmChiA* or *pGADT7-umfly1* on high stringency plates. In contrast, co-transformation of *pGBKT7-ZmChiA* and *pGADT7-umfly1* resulted in yeast growth on high stringency plates, which indicates a physical interaction of UmFly1 and ZmChiA (**Fig. 1d**).

To confirm direct cleavage of ZmChiA by UmFly1, the *U. maydis* fungalysin was produced in *Pichia pastoris.* Cleavage assays using the recombinant UmFly1 resulted in similar ZmChiA processing, as was found for *U. maydis* SG200 culture extracts **(Fig. 1e and Fig. S5a)**. We therefore conclude that enzymatically active UmFly1 directly binds and cleaves maize ZmChiA.

Incubation of ZmChiA with culture filtrate of *U. maydis* results in three products with different sizes. A time course experiment showed that the three cleavage products accumulate in the reaction mixture and over time, the smallest product was accumulating more **(Fig. S5b)**. Western blot analysis detected only full length His-3xHA-ZmChiA, as well as the biggest of the three cleavage products **(Fig. S5c).** To determine the identity of the three ZmChiA cleavage products, gel slices were excised for peptide identification by MS/MS. This approach identified peptides covering between 51.7 to 71.3% of full-length His-3xHA-ZmChiA **(Fig. S6 and Table S2)**. The N-terminal region comprising both tags and the chitin binding domain (CBD) were not covered in all samples. In a next step, we performed differential stable isotope labeling to mark UmFly1-generated neo-N-termini in the cleavage assay. LC-MS/MS revealed cleavage of His-3xHA-ZmChiA between Phe^{39} and Gly^{40} (numbering according to the native ZmChiA sequence), indicating removal of the CBD from the catalytic domain **(Fig. 1f and Fig. S7a-d)**. The theoretical MW of the fragment resulting from this cleavage at Gly^{40} is 25.3 kDa, which corresponds to the fastest migrating ZmChiA cleavage product at ~26 kDa (numbered as 4 in SDS-PAGE in **Fig. 1f**) **(Fig. S7a-d)**. Additional N-termini were detected at Asp^{27} and Asp^{36}, which indicates that UmFly1 cleaves between Tyr and Asp residues in the HA-tag, resulting in

fragments with theoretical MW of 27.5 and 28.6 kDa (numbered as 2 and 3 in SDS-PAGE in **Fig. 1f**), respectively. These fragments correspond with the two cleavage products observed between full-length ZmChiA (numbered as 1 in SDS-PAGE in **Fig. 1f**) and the smallest fragments (numbered as 4 in SDS-PAGE in **Fig. 1f**).

UmFly1 is a virulence factor

To assess a potential biological relevance of UmFly1-mediated ZmChiA cleavage, expression of the *umfly1* gene during maize infection was monitored by qRT-PCR. Similar to maize chitinases, the expression of *umfly1* was also upregulated upon *U. maydis* infection compared to axenic culture (AC) (**Fig. 2a**). Its expression was found to peak at 6 dpi, when also the three maize *chitinases* (*ZmChiA, B* and *C*) show their highest expression level **(Fig. 1a, 2a)**. To characterize the role of *umfly1* in the establishment of maize tumors, seven days-old maize seedlings were inoculated with either *U. maydis* strain SG200, SG200Δumfly1, SG200Δumfly1-C and SG200Δumfly1-C_{mut}. Strikingly, both SG200Δumfly1 and SG200Δumfly1-C_{mut} showed significantly reduced normal tumor formation compared to SG200 at 12 dpi; i.e. SG200Δumfly1 mainly caused chlorosis and small tumor (<2 mm) formation **(Fig. 2b)**. This result identifies UmFly1 as a virulence factor of *U. maydis* and shows that enzymatic activity of UmFly1 is required for the full virulence of the fungus. On the contrary, the SG200Δumfly1-C strain caused disease symptoms similar to SG200, confirming specificity of the phenotype caused by deletion of the *umfly1* gene **(Fig. 2b)**.

Activity assays performed for processed versus full-length ZmChiA showed a significantly reduced activity of ZmChiA after cleavage by UmFly1 (**Fig. 2c**). Thus, one can speculate that the reduced virulence observed for the SG200Δumfly1 mutant could be due to reduced cleavage of ZmChiA. Furthermore, these results are consistent with the *in vitro* cleavage assays, where the SG200Δumfly1 and SG200Δumfly1-C_{mut} strains lost their ZmChiA cleavage activity (**Fig. 1c**). In summary, our findings show that *U. maydis* cleaves the CBD from the catalytic part of the ZmChiA. We suggest that UmFly1-dependent cleavage of the CBD results in a reduced chitin break down efficiency of ZmChiA, which in turn could lead to a reduced virulence of the *U. maydis* SG200Δumfly1 mutant.

UmFly1 is necessary for cell separation of *U. maydis* sporidia

The reduction of virulence in fungal mutants can result from pleiotropic effects, i.e. a generally reduced growth rate or defects in pathogenic development could lead to compromised virulence. We therefore quantified both growth rate and formation of infection structures of the SG200Δumfly1 mutant compared to the progenitor strain SG200. Altogether, these experiments showed that the growth rate in axenic culture, as well as differentiation of infection structures, i.e. the formation of penetration structures (appressoria), were indistinguishable in both SG200Δumfly1 and SG200 strains (**Fig. S8a, b and c**). However, over the course of the characterization of the SG200Δumfly1 strain, we observed a specific developmental phenotype exclusively in the haploid yeast-like phase of *U. maydis*. Microscopic observation of sporidia grown in axenic liquid culture revealed a formation of star-like aggregates, which was not observed in SG200 axenic cultures, indicating a defect in cell separation (**Fig. 3a**). In line with this phenotype, SG200Δumfly1 yeast-like cells showed a faster sedimentation rate compared to SG200 in liquid culture (**Fig. S9**).

U. maydis cell division is accompanied by the formation of a primary and secondary septum between mother and daughter cells. To analyze whether septum formation is disrupted in the SG200Δumfly1 mutant, both SG200 and SG200Δumfly1 dividing cells were stained with calcofluor white (CW) to visualize the chitin cell wall. CW staining revealed that SG200Δumfly1 is not impaired in the formation of the fragmentation zone (**Fig. S8d**). This indicates that the cell division of SG200Δumfly1 is compromised at late stages, particularly during the cell wall degradation step. Recently, Langner *et al*. (2015) have reported a similar phenotype for a double deletion mutant of the endogenous *U. maydis* chitinases *cts1/cts2*. This observation let us to hypothesize that UmFly1 may have an additional role in the regulation of endogenous chitinases of *U. maydis* during cell separation.

To exclude that phenotypic similarity of the *U. maydis* Δ*cts1/cts2* double mutant and SG200Δumfly1 is based on transcriptional down-regulation, gene expression of *cts1*, *cts2*, *cts3*, and *cts4* in both SG200 and SG200Δumfly1 sporidia was analyzed. However, the qRT-PCR results showed no significant differences in the expression levels of the endogenous chitinases between SG200Δumfly1 and the SG200 strain, indicating that UmFly1 is not involved in transcriptional regulation of endogenous chitinases (**Fig. 3b**). Langner *et al*. (2015) showed that Cts1 localizes to the fragmentation zone between mother and daughter cells in *U. maydis* sporidia. To test a possible influence of UmFly1 on the localization of Cts1, the gene sequence

for C-terminally *eGFP* fused *cts1* was expressed under the control of its native promoter in both SG200 and SG200Δumfly1 strains. As a control, the gene for cytoplasmic triple eGFP ($eGFP^3$) was expressed under control of the constitutively active *otef* promoter (Spellig *et al.*, 1996) in SG200 (**Fig 3c**). Southern blot analysis was performed for all strains to confirm single integration of *cts1-eGFP* into the *U. maydis ip*-locus **(Fig. S3e-f)**. Analysis of Cts1-eGFP localization in the SG200 background showed signals in the fragmentation zone between mother and daughter cells, confirming the previous results (Langner *et al.*, 2015). A similar localization of Cts1-eGFP was observed in SG200Δumfly1, suggesting that UmFly1 is not involved in the localization of Cts1-eGFP (**Fig. 3c**).

In contrast, a significant difference between SG200 and SG200Δumfly1 was found for enzymatic activity of native Cts1. While there was no clear difference in Cts1 activity in total cell extracts of both strains (**Fig. 4a**), secreted Cts1 activity was reduced in the SG200Δumfly1 mutant by approximately 50% compared to SG200 (**Fig. 4b**). To test whether this loss of Cts1 activity was due to post-translational modifications, western blot analysis was performed for Cts1-eGFP expressed in SG200 and SG200Δumfly1. In total cell protein extract, full length Cts1-eGFP was detected at the size of 100 kDa in both strains, which is above the calculated size for Cts1-eGFP (82.9 kDa) (**Fig. 4c**). However, while the culture filtrate of SG200Δumfly1 displayed the 100 kDa full length Cts1-eGFP, a band corresponding to 27 kDa only was detected in culture filtrate of the SG200 strain. These results indicate that Cts1-eGFP is C-terminally processed in an UmFly1-dependent manner (**Fig. 4d**). Internal free $eGFP^3$ expressing strain SG200-$eGFP^3$ (Doehlemann *et al.*, 2011) was used as a control to check any internal $eGFP^3$ contamination from cytoplasm to culture filtrate; however, no fluorescence signal was detected in the culture filtrate of the negative control (**Fig. 4d**). From these results, we conclude that UmFly1 is required for processing of secreted Cts1, which in turn is necessary for proper cell separation of *U. maydis* sporidia.

To determine the identity of UmFly1-dependent cleavage products of Cts1-GFP, samples were analyzed by MS/MS **(Fig. 4e)**. Mapping of tryptic peptides showed good coverage of the GH18 domain and the eGFP tag **(Fig. 4e, Fig. S10 and Table S2)**. The first 127 residues of recombinant Cts1-GFP were not covered, which could be explained by a lack of tryptic cleavage sites in this sequence. Differential stable isotope labeling was used to determine UmFly1-dependent N-termini in Cts1-GFP. This approach identified two cleavage sites: one site between

Gln[96] and Asn[97] amino acid (numbering according to the native Cts1 sequence), removing 96 aa N-terminal of the GH18 catalytic domain, and a second site between Ala[519] and Thr[520] in the linker region between Cts1 and the C-terminal eGFP tag **(Fig. 4e and Fig. S11a-b)**. Cleavage at both sites predicts a Cts1 fragment of 45.8 kDa, consistent with the observation of a faint band on the Coomassie-stained SDS-PAGE in this region that appeared only after incubation with SG200 culture filtrate **(Fig. 4e)**. Taken together, this approach shows cleavage of Cts1 by UmFly1 where the removal of an N-terminal 96 aa peptide might lead to post-translational activation of Cts1.

Heterologous complementation of the SG200Δumfly1 mutant separates Fly1 functions

Fly1 is well conserved among fungi, including plant and animal pathogenic fungi, epiphytic, and saprophytic fungi **(Fig. S1)** (Li & Zhang, 2014; Sanz-Martin *et al.*, 2016). To analyze whether an orthologue of UmFly1 from a related, but not maize-pathogenic fungal species can complement both the axenic phenotype and the virulence defect of SG200Δumfly1, the deletion mutant was complemented with the *fly1* coding sequence from *Moesziomyces sp*. (Thines *et al.*, 2009; Wang *et al.*, 2015; Kruse *et al.*, 2017). This fungal species belongs to the *Ustilaginales* and has been identified and isolated as an epiphytic fungus from *Arabidopsis thaliana* leaves, where it was associated with the pathogenic oomycete *Albugo laibachii* (Agler *et al.*, 2016). For proper expression of MoFly1 in *U. maydis*, the coding region was expressed under the control of the native *umfly1* promoter. In addition, its N-terminal signal peptide was substituted by that of UmFly1 for proper secretion in *U. maydis* **(Fig. S12)**. To generate the strain SG200Δumfly1-mofly1, the construct for *mofly1* expression was integrated into the *U. maydis ip*-locus (Loubradou *et al.*, 2001). After confirmation of a single integration of the construct by Southern blot analysis **(Fig. S3d)**, microscopic observation was performed to check whether *mofly1* can rescue the cell separation defect of SG200Δumfly1. Microscopic observation results revealed SG200 like growth of SG200Δumfly1-mofly1 sporidia, showing that expression of *mofly1* fully complements the axenic growth phenotype (**Fig. 5a**). Consistent with this result, Cts1-eGFP processing activity of SG200Δumfly1-mofly1 was similar to SG200 culture filtrate (**Fig. 5b**). Together, this shows that MoFly1 can fully complement UmFly1 during the yeast-like growth phase of *U. maydis* in axenic culture. To test whether the same is true for the virulence function of UmFly1, seven days-old maize seedlings were infected with the *U. maydis* strains SG200,

SG200Δumfly1, SG200Δumfly1-C and SG200Δumfly1-mofly1 and scored for tumor formation at 12 dpi. Interestingly, SG200Δumfly1-mofly1 showed only a partially complemented virulence compared to the SG200Δumfly1-C, indicating that MoFly1 is not fully functional as a virulence factor in *U. maydis* (**Fig. 5c**). Consistent with this phenotype, also Fly1-dependent cleavage of ZmChiA appeared to be only partial in presence of the *Moesziomyces sp.* homolog compared to UmFly1 (**Fig. 5d**). Based on these results we conclude that of the MoFly1 does not have the same function of UmFly1 during maize infection.

Discussion

Plant chitinases are an important part of the first layer of plant immunity. They target a major component of the fungal cell wall to restrict fungal growth and enable the perception of released chitin fragments by pattern recognition receptors (PRRs) (Schlumbaum *et al.*, 1986; Iseli *et al.*, 1993; Kaku *et al.*, 2006; Silipo *et al.*, 2010). Since the fungal cell wall plays an essential role for the fitness of all fungi, pathogens evolved different strategies to avoid the deleterious effect of host cell wall degrading enzymes (Vander *et al.*, 1998; van den Burg *et al.*, 2006; de Jonge *et al.*, 2010; Naumann *et al.*, 2011; Jashni *et al.*, 2015; Sanz-Martin *et al.*, 2016). Although *U. maydis* is a well-studied model system, it is still unknown how this biotrophic pathogen counteracts host chitinases. This study shows how *U. maydis* modulates both host- and endogenous chitinase activities during pathogenic development and saprophytic yeast growth, respectively.

Homology based BLAST search performed with *F. verticillioides* FvFly1, a plant chitinase-cleaving fungalysin metalloprotease (Naumann, 2011), revealed the presence of a single copy gene in *U. maydis* encoding the UmFly1 fungalysin. The expression of *umfly1* in *U. maydis* is strongly induced upon maize infection, reflecting its importance to establish and maintain the biotrophic interaction. Consistent with this, Sanz-Martin *et al*. (2016) have shown that *cgfl*, a fungalysin encoding gene of *C. graminicola*, is specifically up-regulated during the biotrophic phase of the infection process and it is down-regulated upon the switch from the biotrophic phase to the necrotrophic phase. These results suggest that the biotrophic pathogen *U. maydis* and the hemi-biotroph *C. graminicola* both require fungalysin particularly during biotrophic growth, when the fungus depends on suppression of host defense. Significant virulence reduction in the SG200Δumfly1 mutant also confirms the relevance of fungalysin in the *U. maydis*-maize interaction. Consistently, *cgfl* of *C. graminicola* was also found to be involved in virulence

during maize infection (Sanz-Martin *et al.*, 2016). The observed reduction of ZmChiA cleavage activity, as well as the reduced virulence both in the SG200Δumfly1 mutant and the active site mutant (SG200Δumfly1-C_{mut}), indicate that the enzymatic activity of UmFly1 is required for the cleavage of maize ZmChiA, and consequently for *U. maydis* virulence. Interaction of UmFly1 with ZmChiA in the Y2H assay and cleavage of ZmChiA with *P. pastoris*-produced UmFly1 indicate physical action of UmFly1 with ZmChiA. The UmFly1-mediated reduction of ZmChiA efficiency in the degradation of fungal chitin might dampen plant defense responses that are induced by the release of chitin fragments from the fungal cell wall. Thus, UmFly1 represents an alternative strategy to fungal chitin binding effectors, such as Avr4 and Ecp6 from *C. fulvum* (van den Burg *et al.*, 2006; de Jonge *et al.*, 2010). Presence of the same chitinase detoxification strategy in several other maize pathogens, including *F. verticillioides* and *C. graminicola*, indicates that truncation of chitinases by Fly1 might be an evolutionary ancient strategy (Naumann *et al.*, 2011; Jashni *et al.*, 2015; Sanz-Martin *et al.*, 2016).

Previous studies described that FvFly1 cleaves ZmChiA at the hinge domain to release the chitin binding (CBD) and hydrolase domains as byproducts (Naumann, 2011; Naumann *et al.*, 2011; Jashni *et al.*, 2015). Consistently, this study also showed that *U. maydis* cleaves ZmChiA at the CBD (between Phe^{39} and Gly^{40}). Recently, Jashni *et al*. (2015) also identified the same cleavage site for tomato SlChi1 after cleavage with *F. oxysporum* FoMep1 (also a Fly1 homolog). Moreover, they also reported that the *F. oxysporum* f.sp. *lycopersici* metalloprotease FoMep1 and a serine protease (FoSep1) have a synergetic effect on tomato chitinase cleavage and on fungal virulence as well (Jashni *et al.*, 2015). Only double deletion mutants of *fomep1*/*fosep1* showed a significant virulence defect for *F. oxysporum* f.sp. *lycopersici* (Jashni *et al.*, 2015). Contrary, in *U. maydis* the deletion of *umfly1* alone already results in a loss of ZmChiA cleavage activity and a reduced virulence of the fungus, indicating the importance of *umfly*1 for interaction with the host plant. Consistent with these results, *cgfl* of *C. graminicola* is also involved in virulence during maize infection (Sanz-Martin *et al.*, 2016). Additionally, *U. maydis* also contains a single copy gene orthologous to *fosep1*. However, whether this *U. maydis* serine protease is also involved in chitinase cleavage or in fungal virulence remains elusive and will be subject of future studies.

In addition to an impaired ZmChiA cleavage activity and the reduced virulence, the SG200Δumfly1 mutant is also impaired in cell separation during the yeast-like growth phase in

axenic culture. During cell growth, fungi remodel their cell wall by fine-tuning the activity of endogenous fungal chitinases, such as Cts1 and Cts2 in *U. maydis* (Langner *et al.*, 2015). Langner *et al*. (2015) reported that the double gene deletion of *cts1* and *cts2* (Δ*cts1/2*) in *U. maydis* leads to a defect in cell separation and thus formation of multicellular aggregates in axenic culture. Interestingly, this axenic phenotype perfectly resembles the one of SG200Δumfly1. This led us to hypothesize that UmFly1 might also be associated with the regulation of *U. maydis* endogenous fungal chitinases. Like the double Δ*cts1/2* mutant, the SG200Δumfly1 mutant showed no defects in formation of the separation zone (Langner *et al.*, 2015). Furthermore, Cts1 is still localized between the primary and secondary septum in SG200Δumfly1 in order to degrade the remnant chitin in the separation zone (Langner *et al.*, 2015). However, activity assays performed in culture supernatants of the SG200Δumfly1 revealed that the Cts1 activity was reduced by 50% in the mutant compared to the SG200 strain. This indicates that UmFly1 is also involved in posttranslational regulation of endogenous chitinase activity. Consistent with this result, our MS/MS analysis revealed that UmFly1 is required for removal of the 96 N-terminal amino acids of Cts1. We speculate that this processing might lead to an activation of Cts1 being required to confer proper cell separation. However, the exact mechanism of Cts1 and its role in cell separation of *U. maydis* will be addressed in future studies. Since the cell separation defect previously was observed only in the double Δ*cts1/2* mutant (Langner *et al.*, 2015), one can further speculate that UmFly1 at least participates in the activation of both Cts1 and Cts2. Although both the Δ*cts1/2* and the SG200Δumfly1 mutants have the same *in vitro* phenotype, only the SG200Δumfly1 mutant is reduced in virulence. Even deletion of all four predicted *U. maydis* chitinases in the quadruple *cts1/2/3/4* mutant did not result in a detectable reduction of virulence (Langner *et al.*, 2015). Despite the impaired cell separation phenotype of both Δ*umfly1* and quadruple Δ*cts1/2/3/4* mutants (Langner *et al.*, 2015), none of these mutants showed any defect in growth rate or filamentation, respectively. This indicates that chitin remodeling by the endogenous chitinases (*cts1-4*) is not required for filament morphogenesis and pathogenic development of *U. maydis*. Therefore, the situation in *U. maydis* is different from what has been described previously for several filamentous fungi. In both *Neurospora crassa* and *Aspergillus nidulans*, endogenous chitinases are important for hyphal growth (Takaya *et al.*, 1998; Tzelepis *et al.*, 2012). Consistent with our data, Slavokhotova *et al*., (2014) showed that the inhibition of a *F. verticillioides* fungalysin by a hevein-like peptide from

463 wheat results in the inhibition of hyphal elongation, indicating that fungalysin plays a role in
464 fungal development.
465 Phylogenetic analysis performed for Fly1 showed that putative Fly1 homologs are conserved in
466 diverse fungal lineages that have diverse lifestyles, including saprophytes, as well as plant and
467 animal pathogens (Li & Zhang, 2014). This suggests that fungalysin proteins are not necessarily
468 associated with pathogenicity. Consistently, UmFly1 is not only required for host chitinase
469 cleavage, but also for activation of the endogenous chitinase Cts1 in the *U. maydis* strain SG200.
470 The latter function, however, is not relevant for plant infection. Recently, Takahara *et al*., (2016)
471 also reported a dual role for a *Colletotrichum higginsianum* LysM effector protein, which is
472 involved in both suppression of chitin-triggered immunity and required for appressorium-
473 mediated host penetration. Another recent report also showed that Sntox1 of the necrotrophic
474 fungal pathogen *Parastagonospora nodorum* was found being a dual-function protein that
475 facilitates infection inducing cell death and protecting the fungal hypha from wheat chitinases
476 (Liu *et al*., 2016). However, unlike the dual function of UmFly1, which is associated with both
477 saprobic and pathogenic growth, in these two reports the dual function of the proteins is
478 associated only with pathogenic life style (Takahara *et al*., 2016; Liu *et al*., 2016). One could
479 speculate that the initial function of Fly1 proteins was to regulate endogenous chitinase activity
480 for proper cell separation during saprobic growth. However, during association of *U. maydis*
481 with its host plant, UmFly1 could have gained an additional function to counter host chitinases,
482 which supports host infection, i.e. results in elevated tumor formation (and consequently
483 increased formation of teliospores). To test this hypothesis, we have performed a
484 complementation study with the UmFly1 homolog from the related smut fungus
485 *Moesziomyces* sp., which has been identified as an epiphyte of *Arabidopsis thaliana* (Wang *et*
486 *al.*, 2015). Although *mofly1* fully complements the SG200Δumfly1 phenotype in axenic culture,
487 it only partially complements its virulence defect on maize. To further challenge this hypothesis
488 in an evolutionary context, future studies may involve testing additional homologs from different
489 related pathogens (such as the maize and sorghum anther smut *Sporisorium reilianum*, or the
490 barley covered smut *Ustilago hordei*), as well as saprophytic species. Within some animal fungal
491 pathogens, M36 fungalysin metalloproteases are described to undergo dynamic evolutionary
492 changes with significant positive selection, which could possibly be important in host-immune
493 system interactions (Li & Zhang, 2014). This suggests that fungal species share the conserved

endogenous function of the M36 fungalysin metalloproteases, while its virulence function, which is seen in *U. maydis* and several other fungal species, is specific for pathogens. Consistent with this, culture filtrate of *C. fulvum* cannot cleave CBD of chitinases (although *C. fulvum* has a *Fly1* homolog) (Jashni *et al.*, 2015). This suggests that CfFly1 has not adapted to chitinase cleavage, since *C. fulvum* already has Avr4 and Ecp6 to protect the fungus against negative effects of host chitinases (de Wit *et al.*, 2012; Jashni *et al.*, 2015). One can speculate that CfFly1 may be primarily involved in cell wall modification of this fungus. On the contrary, culture filtrates from some other tomato pathogens, such as *F. oxysporum, V. dahliae* and *B. cinerea* that do not have Avr4 homologs, show chitinase cleavage activity (Jashni *et al.*, 2015). Moreover, some fungi have genes for both LysM effectors and Fly1-like proteins, and both genes can be involved in virulence (Takahara *et al*., 2016; Sanz-Martin *et al*., 2016). However, while two LysM proteins in *Colletotrichum higginsianum* are required for suppression of recognition of released chitin fragments by the host plant (Takahara *et al*., 2016), *C. graminicola* Fly1 (Cgfl) is involved in reduction of host chitinase activity (Sanz-Martin *et al*., 2016).

This study discovers a regulator for the posttranslational activation of fungal chitinases in *U. maydis*. In addition to regulation of the endogenous chitinase Cts1 during *U. maydis* cell separation in axenic culture, UmFly1 also confers cleavage and deactivation of host chitinases to promote virulence. While functions of microbial effectors are generally linked to disease establishment, our data imply a broader function for UmFly1 beyond the interaction with the host plant. We hypothesize that during co-evolution with its maize host, *U. maydis* adapted its endogenous chitinase regulating machinery to cleave and deactivate host chitinases, which increased its ability to suppress host immunity and consequently increased its virulence capacity. Overall, this study provides new insight in how effectors could evolve from previously existing proteins to better adapt to the host immune machinery and thereby support virulence.

Acknowledgments

This work was supported by the Cluster of Excellence on Plant Science (CEPLAS). Kerstin Schipper receives funding from the SFB1208 Membrane Dynamics and Identity. We thank Katharina Lentz for providing the sequence of MoFly1. We thank Regine Kahmann for general support and fruitful discussions. We acknowledge Sachin Teotia for his help with cloning of maize chitinase genes and Thorsten Langner for support with chitinase activity assays.

Author Contribution

BÖ and GD conceived the project. BÖ, BK, DH, RW carried out transformation and disease assays; protein production and Y2H assay; JA carried out chitinase activity assay; AP carried out mass spectrometry analyses; PFH and KS were involved in interpretation of the data; BÖ wrote the manuscript with input from all authors.

References

Agler MT, Ruhe J, Kroll S, Morhenn C, Kim S-T, Weigel D, Kemen EM. 2016. Microbial hub taxa link host and abiotic factors to plant microbiome variation. *PLOS Biology* **14**(1): e1002352.

Bolton MD, Van Esse HP, Vossen JH, De Jonge R, Stergiopoulos I, Stulemeijer IJE, Van Den Berg GCM, Borrás-Hidalgo O, Dekker HL, De Koster CG, et al. 2008. The novel *Cladosporium fulvum* lysin motif effector Ecp6 is a virulence factor with orthologues in other fungal species. *Mol Microbiol* **69**(1): 119-136.

Brouta F, Descamps F, Monod M, Vermout S, Losson B, et al. 2002. Secreted metalloprotease gene family of *Microsporum canis*. *Infection and Immunity* **70:** 5676-5683.

de Jonge R, van Esse HP, Kombrink A, Shinya T, Desaki Y, Bours R, van der Krol S, Shibuya N, Joosten MH, Thomma BP. 2010. Conserved fungal LysM effector Ecp6 prevents chitin-triggered immunity in plants. *Science* **329**(5994): 953-955.

de Wit PJ, van der Burgt A, Okmen B, Stergiopoulos I, Abd-Elsalam KA, Aerts AL, Bahkali AH, Beenen HG, Chettri P, Cox MP, et al. 2012. The genomes of the fungal plant pathogens *Cladosporium fulvum* and *Dothistroma septosporum* reveal adaptation to different hosts and lifestyles but also signatures of common ancestry. *PLoS Genet* **8**(11): e1003088.

Doehlemann G, Reissmann S, Assmann D, Fleckenstein M, Kahmann R. 2011. Two linked genes encoding a secreted effector and a membrane protein are essential for *Ustilago maydis*-induced tumour formation. *Mol Microbiol* **81**(3): 751-766.

Doehlemann G, Wahl R, Horst RJ, Voll LM, Usadel B, Poree F, Stitt M, Pons-Kühnemann J, Sonnewald U, Kahmann R, et al. 2008. Reprogramming a maize plant:

transcriptional and metabolic changes induced by the fungal biotroph *Ustilago maydis*. *Plant Journal* **56**(2): 181-195.

Duplessis S, Cuomo CA, Lin Y-C, Aerts A, Tisserant E, Veneault-Fourrey C, Joly DL, Hacquard S, Amselem J, Cantarel BL, et al. 2011. Obligate biotrophy features unraveled by the genomic analysis of rust fungi. *Proceedings of the National Academy of Sciences* **108**(22): 9166-9171.

El Gueddari NE, Rauchhaus U, Moerschbacher BM, Deising HB. 2002. Developmentally regulated conversion of surface-exposed chitin to chitosan in cell walls of plant pathogenic fungi. *New Phytologist* **156**: 103-112.

Hemetsberger C, Herrberger C, Zechmann B, Hillmer M, Doehlemann G. 2012. The *Ustilago maydis* effector Pep1 suppresses plant immunity by inhibition of host peroxidase activity. *PLoS Pathog* **8**(5): e1002684.

Henrissat B, Davies G. 1997. Structural and sequence-based classification of glycoside hydrolases. *Current Opinion in Structural Biology* **7**(5): 637-644.

Huynh QK, Hironaka CM, Levine EB, Smith CE, Borgmeyer JR, Shah DM. 1992. Antifungal proteins from plants. Purification, molecular cloning, and antifungal properties of chitinases from maize seed. *J Biol Chem* **267**(10): 6635-6640.

Iseli B, Boller T, Neuhaus JM. 1993. The N-terminal cysteine-rich domain of tobacco class i chitinase is essential for chitin binding but not for catalytic or antifungal activity. *Plant Physiol* **103**(1): 221-226.

Jashni MK, Dols IHM, Iida Y, Boeren S, Beenen HG, Mehrabi R, Collemare J, de Wit PJGM. 2015. Synergistic action of a metalloprotease and a serine protease from *Fusarium oxysporum* f. sp. *lycopersici* cleaves chitin-binding tomato chitinases, reduces their antifungal activity, and enhances fungal virulence. *Molecular Plant-Microbe Interactions* **28**(9): 996-1008.

Kaku H, Nishizawa Y, Ishii-Minami N, Akimoto-Tomiyama C, Dohmae N, Takio K, Minami E, Shibuya N. 2006. Plant cells recognize chitin fragments for defense signaling through a plasma membrane receptor. *Proceedings of the National Academy of Sciences of the United States of America* **103**(29): 11086-11091.

Kämper J, Kahmann R, Bölker M, Ma LJ, Brefort T, Saville BJ, Banuett F, Kronstad JW, Gold SE, Müller O, et al. 2006. Insights from the genome of the biotrophic fungal plant pathogen *Ustilago maydis*. *Nature* **444**(7115): 97-101.

Kasprzewska A. 2003. Plant chitinases--regulation and function. *Cell Mol Biol Lett* **8**(3): 809-824.

Kruse J, Doehlemann G, Kemen E, Thines M. 2017. Asexual and sexual morphs of *Moesziomyces* revisited. *IMA Fungus* **8**(1): 117-129.

Kuranda MJ, Robbins PW. 1991. Chitinase is required for cell separation during growth of *Saccharomyces cerevisiae*. *J Biol Chem* **266**: 19758-19767.

Langner T, Gohre V. 2016. Fungal chitinases: function, regulation, and potential roles in plant/pathogen interactions. *Curr Genet* **62**(2): 243-254.

Langner T, Ozturk M, Hartmann S, Cord-Landwehr S, Moerschbacher B, Walton JD, Gohre V. 2015. Chitinases are essential for cell separation in *Ustilago maydis*. *Eukaryot Cell* **14**(9): 846-857.

Leake JR, Read DJ. 1990. Chitin as a Nitrogen-source for mycorrhizal fungi. *Mycol Res* **94**: 993-995.

Li J, Zhang K-Q. 2014. Independent expansion of zincin metalloproteinases in Onygenales fungi may be associated with their pathogenicity. *PLoS One* **9**(2): e90225.

Liu Z, Gao Y, Kim YM, Faris JD, Shelver WL, de Wit PJ, Xu SS, Friesen TL. 2016. SnTox1, a *Parastagonospora nodorum* necrotrophic effector, is a dual-function protein that facilitates infection while protecting from wheat-produced chitinases. *New Phytologist* **211**(3):1052-64. doi: 10.1111.

Livak KJ, Schmittgen TD. 2001. Analysis of relative gene expression data using real-time quantitative PCR and the $2^{-\Delta\Delta CT\ method}$. *Methods* **25**(4): 402-408.

Lo Presti L, Lanver D, Schweizer G, Tanaka S, Liang L, Tollot M, Zuccaro A, Reissmann S, Kahmann R. 2015. Fungal effectors and plant susceptibility. *Annu Rev Plant Biol* **66**: 513-545.

Loubradou G, Brachmann A, Feldbrügge M, Kahmann R. 2001. A homologue of the transcriptional repressor Ssn6p antagonizes cAMP signalling in *Ustilago maydis*. *Mol Microbiol* **40**(3): 719-730.

Marshall R, Kombrink A, Motteram J, Loza-Reyes E, Lucas J, Hammond-Kosack KE, Thomma BPHJ, Rudd JJ. 2011. Analysis of two in planta expressed lysm effector homologs from the fungus *Mycosphaerella graminicola* reveals novel functional properties and varying contributions to virulence on wheat. *Plant Physiol* **156**(2): 756-769.

Mentlak TA, Kombrink A, Shinya T, Ryder LS, Otomo I, Saitoh H, Terauchi R, Nishizawa Y, Shibuya N, Thomma BPHJ, et al. 2012. Effector-mediated suppression of chitin-triggered immunity by *Magnaporthe oryzae* is necessary for rice blast disease. *Plant Cell* **24**(1): 322-335.

Mueller AN, Ziemann S, Treitschke S, Assmann D, Doehlemann G. 2013. Compatibility in the *Ustilago maydis*-maize interaction requires inhibition of host cysteine proteases by the fungal effector Pit2. *PLoS Pathog* **9**(2): e1003177.

Naumann TA. 2011. Modification of recombinant maize ChitA chitinase by fungal chitinase-modifying proteins. *Mol Plant Pathol* **12**(4): 365-372.

Naumann TA, Wicklow DT. 2013. Chitinase modifying proteins from phylogenetically distinct lineages of Brassica pathogens. *Physiological and Molecular Plant Pathology* **82**: 1-9.

Naumann TA, Wicklow DT, Price NP. 2011. Identification of a chitinase-modifying protein from *Fusarium verticillioides*: truncation of a host resistance protein by a fungalysin metalloprotease. *J Biol Chem* **286**(41): 35358-35366.

Sambrook J, Fritsch EF, Maniatis T. 1989. Molecular cloning: a laboratory manual. *Cold Spring Harbor Laboratory, Cold Spring Harbor, New York.*

Sanz-Martin JM, Pacheco-Arjona JR, Bello-Rico V, Vargas WA, Monod M, Diaz-Minguez JM, Thon MR, Sukno SA. 2016. A highly conserved metalloprotease effector enhances virulence in the maize anthracnose fungus *Colletotrichum graminicola*. *Mol Plant Pathol* **17**(7): 1048-1062.

Schlumbaum A, Mauch F, Vogeli U, Boller T. 1986. Plant chitinases are potent inhibitors of fungal growth. *Nature* **324**(6095): 365-367.

Schulz B, Banuett F, Dahl M, Schlesinger R, Schäfer W, Martin T, Herskowitz I, Kahmann R. 1990. The *b* alleles of *U. maydis*, whose combinations program pathogenic development, code for polypeptides containing a homeodomain-related motif. *Cell* **60**(2): 295-306.

Shibuya N, Minami E. 2001. Oligosaccharide signalling for defence responses in plant. *Physiological and Molecular Plant Pathology* **59**(5): 223-233.

Shoresh M, Harman GE. 2008. Genome-wide identification, expression and chromosomal location of the genes encoding chitinolytic enzymes in *Zea mays*. *Molecular Genetics and Genomics* **280**(2): 173.

Silipo A, Erbs G, Shinya T, Dow JM, Parrilli M, Lanzetta R, Shibuya N, Newman M-A, Molinaro A. 2010. Glyco-conjugates as elicitors or suppressors of plant innate immunity. *Glycobiology* **20**(4): 406-419.

Slavokhotova AA, Naumann TA, Price NPJ, Rogozhin EA, Andreev YA, Vassilevski AA, Odintsova TI. 2014. Novel mode of action of plant defense peptides – hevein-like antimicrobial peptides from wheat inhibit fungal metalloproteases. *FEBS Journal* **281**(20): 4754-4764.

Spellig T, Bottin A, Kahmann R. 1996. Green fluorescent protein (GFP) as a new vital marker in the phytopathogenic fungus *Ustilago maydis*. *Mol Gen Genet* **252**(5): 503-509.

Takahara H, Hacquard S, Kombrink A, Hughes HB, Halder V, Robin GP, et al. 2016. *Colletotrichum higginsianum* extracellular LysM proteins play dual roles in appressorial function and suppression of chitin-triggered plant immunity. *New Phytologist* **211**:1323-1337. pmid:27174033.

Takaya N, Yamazaki D, Horiuchi H, Ohta A, Takagi M. 1998. Cloning and characterization of a chitinase-encoding gene (*chiA*) from *Aspergillus nidulans*, disruption of which decreases germination frequency and hyphal growth. *Biosci Biotechnol Biochem* **62**(1): 60-65.

Thines M, Choi YJ, Kemen E, Ploch S, Holub EB, Shin HD, Jones JDG. 2009. A new species of *Albugo* parasitic to *Arabidopsis thaliana* reveals new evolutionary patterns in white blister rusts (Albuginaceae). *Persoonia* **22**: 123-128.

Tzelepis GD, Melin P, Jensen DF, Stenlid J, Karlsson M. 2012. Functional analysis of glycoside hydrolase family 18 and 20 genes in *Neurospora crassa*. *Fungal Genetics and Biology* **49**(9): 717-730.

van den Burg HA, Harrison SJ, Joosten MHAJ, Vervoort J, de Wit PJGM. 2006. *Cladosporium fulvum* Avr4 protects fungal cell walls against hydrolysis by plant

chitinases accumulating during infection. *Molecular Plant-Microbe Interactions* **19**(12): 1420-1430.

van Esse HP, Bolton MD, Stergiopoulos I, de Wit PJGM, Thomma BPHJ. 2007. The chitin-binding *Cladosporium fulvum* effector protein avr4 is a virulence factor. *Molecular Plant-Microbe Interactions* **20**(9): 1092-1101.

Vander P, Vårum KM, Domard A, Eddine El Gueddari N, Moerschbacher BM. 1998. Comparison of the ability of partially N-acetylated chitosans and chitooligosaccharides to elicit resistance reactions in wheat leaves. *Plant Physiol* **118**(4): 1353-1359.

Veneault-Fourrey C, Commun C, Kohler A, Morin E, Balestrini R, Plett J, Danchin E, Coutinho P, Wiebenga A, de Vries RP, et al. 2014. Genomic and transcriptomic analysis of *Laccaria bicolor* CAZome reveals insights into polysaccharides remodelling during symbiosis establishment. *Fungal Genet Biol* **72**: 168-181.

Wang QM, Begerow D, Groenewald M, Liu XZ, Theelen B, Bai FY, Boekhout T. 2015. Multigene phylogeny and taxonomic revision of yeasts and related fungi in the Ustilaginomycotina. *Studies in Mycology* **81**: 55-83.

Supporting information captions

Additional Supporting Information may be found online in the Supporting Information tab for this article:

Fig. S1 Amino acid alignment of UmFly1, MoFly1 and FvFly1.

Fig. S2 Phylogenetic tree analysis of the Fly1 protein.

Fig. S3 Southern Blot analysis for the confirmation of gene replacement and single insertion events.

Fig. S4 Western Blot analysis for the confirmation of protein production and stability in yeast cell for Y2H assay.

Fig. S5 Cleavage of N-terminally His and HA tagged ZmChiA recombinant protein by culture filtrate of *UmFly1* expressing *Pichia pastoris* and *Ustilago maydis*.

Fig. S6 Tryptic peptides recovered after in-gel digest of the bands in the cleavage assay mapped to the sequence of His-3xHA-ZmChiA.

Fig. S7 N-terminal peptides identified after incubation of His-3XHA-ZmChiA with UmFly1 culture filtrate.

Fig. S8 Fitness of the of SG200Δumfly1 mutant in comparison to the *Ustilago maydis* SG200 strain.

Fig. S9 Sedimentation of SG200Δumfly1-C compared to the *Ustilago maydis* progenitor strain SG200.

Fig. S10 Tryptic peptides recovered after in-gel digest of the bands in the cleavage assay mapped to the sequence of Cts1-GFP.

Fig. S11 N-terminal peptides identified after incubation of Cts1-GFP with UmFly1 culture filtrate.

Fig. S12 Schematic illustration of complementation constructs.

Table S1 Plasmids and primers used in this study.

Table S2 ZmChiA and Cts1-GFP peptides identified in MS/MS analysis.

Methods S1. The experiments performed in this manuscript have been explained in more detail.

Figure legends

Fig. 1 (a) Expression profile of *Zea mays* chitinase genes in mock and *Ustilago maydis*-infected maize leaves. Quantitative real-time PCR (qRT-PCR) was performed to assess the expression profiles of *ZmChiA*, *ZmChiB* and *ZmChiC*. Expression levels were normalized using the maize *GAPDH* (glyceraldehyde-3-P dehydrogenase) gene. A one way ANOVA analysis followed by Dunnett's multiple comparisons test was performed. Significant differences compared to mock samples are shown with asterisk (** P<0,005). Error bars represent standard deviation of three biological replicates. **(b-c)** Cleavage of N-terminally His and HA tagged ZmChiA recombinant protein by culture filtrate of *Ustilago maydis*. Recombinant ZmChiA was produced and purified using the *Pichia pastoris* protein expression system. 15 µg of purified ZmChiA were incubated with 30 µl of 50 times concentrated culture filtrate of *U. maydis* SG200, SG200Δumfly1, UmFly1 complementation (SG200Δumfly1-C) and UmFly1 active site mutant (SG200Δumfly1-C_{mut}) strains, which was isolated from *U. maydis* grown in $YEPS_{light}$ liquid medium (OD_{600}1.0). The mixture was incubated at 28°C for 18 hours. The cleavage of ZmChiA was visualized by coomassie blue staining (b) and sypro ruby staining (c) of the SDS gel. ZmChiA incubated with non-inoculated $YEPS_{light}$ (50 times concentrated) was used as a negative control. The predicted MW of ZmChiA is 32 kDa. **(d)** *In vivo* interaction of ZmChiA and UmFly1 in the yeast-2-hybrid system. The *pGBKT7-ZmChiA* construct was co-transformed with *pGADT7-umfly1* or with empty vector controls into *Saccharomyces cerevisiae* AH109 strain. Different dilutions (10^0, 10^{-1}

and 10^{-2}) of each sample were spotted on low (-Leu and -Trp) and high (-Leu, -Trp, -Ade and -His) stringency plates. Pictures were taken after 5 days of incubation at 28°C. Growth on high stringency plates indicates physical interaction of the proteins within the cell. **(e)** Cleavage of N-terminally His-3xHA tagged ZmChiA by *P. pastoris*-produced, C-terminally His-tagged UmFly1. 15 µg of His-HA-ZmChiA was incubated with 50 µl of UmFly1-His and mixture was incubated at 28°C for 5 h. Coomassie blue staining was performed for the visualization of ZmChiA cleavage. The predicted MW of His-3xHA-ZmChiA is 31.8 kDa and UmFly1-His is 107 kDa. **(f)** In order to determine the cleavage sites, the cleaved products of ZmChiA after incubation with *U. maydis* culture filtrate were identified via MS/MS analysis. While the band labeled with number '1' represents the full length ZmChiA, the 2-4 numbered bands represent the cleaved ZmChiA in SDS-PAGE stained with Coomassie blue. The schematic diagram depicts structure and cleavage sites (arrowheads) of the full length protein (band '1', top panel, 31.8kDa) and the three cleavage products (corresponding to bands '2' to '4', three lower panels, 28.6kDa, 27.6kDa and 25.3kDa, respectively).

Fig. 2 (a) Expression profile of *Ustilago maydis umfly1* in axenic culture (AC) and during maize infection. Quantitative real-time PCR (qRT-PCR) was performed to assess the expression profile of *umfly1*. Expression levels were normalized by using *U. maydis ppi* (*peptidylprolyl isomerase*) gene. One way ANOVA analysis followed by Dunnett's multiple comparisons test was performed. Significant differences compared to AC are shown with an asterisk (* P<0,05 and *** P<0,0001). Error bars represent standard deviation of three biological replicates. **(b)** SG200Δumfly1 mutant showed reduced virulence on maize compared to the SG200 strain. Disease rating of the symptoms caused by SG200Δumfly1 and SG200Δumfly1-C_{mut} in comparison with SG200 and *umfly1* complementation (SG200Δumfly1-C) strains at 12 dpi. The SG200Δumfly1 mutant shows significantly reduced normal tumor formation compared to *U. maydis* SG200 and complementation strains on Early Golden Bantam (EGB) maize lines. The virulence assay was performed in three independent biological replicates. A *chi*-squared test was performed to show significant differences (P<0,0001). n= number of infected maize seedlings. **(c)** Relative chitinase activity assay. After incubation of 300 µl ZmChiA (10 mM NaAcetate pH: 5.3) with 300 µl of SG200 and SG200Δumfly1 cell free culture filtrate and $YEPS_{light}$ medium (concentrated) at 28°C for 12 hours, 600 µl of Chitin-Azur (10 mg/1800 µl K-Phosphate Buffer

pH: 6.0) were incubated with 300 µl of reaction mix at 37°C for overnight, to check whether cleaved ZmChiA has less activity compared to full length. The absorbance was measured at 560 nm. Significant differences compared to full length ZmChiA are shown with asterisks (*** *P*<0,0003). Error bars represent standard deviation of three biological replicates.

Fig. 3 (a) SG200Δumfly1 mutants show a cell separation defect in liquid axenic culture. While *U. maydis* SG200 shows the characteristic yeast-like growth with polar budding of daughter cells, the SG200Δumfly1 mutant forms clumps in liquid culture. Scale bars indicate 20 µm. **(b)** Expression profile of endogenous chitinases in *Ustilago maydis* SG200 and SG200Δumfly1 strains grown in axenic culture. Quantitative real-time PCR was performed to assess the expression profiles of endogenous chitinases, such as *cts1*, *cts2*, *cts3* and *cts4*. Expression levels were normalized using the *U. maydis ppi* (*peptidylprolyl isomerase*) gene. A one way ANOVA analysis followed by Dunnett's multiple comparisons test was performed. There are no significant differences in chitinase expressions between *U. maydis* SG200 and SG200Δumfly1 strains. Error bars represent standard deviation of three biological replicates. **(c)** Microscopic observation of the localization of Cts1-eGFP in *Ustilago maydis* SG200 and SG200Δumfly1 strains. *cts1-eGFP* expressing *U. maydis* SG200 (middle) and SG200Δumfly1 (right) were stained with calcofluor white (CW) and subsequently pictures were taken with bright field (DIA, top), eGFP filter (second line) and DAPI filter (CW, third line). Yellow arrows show the localization of Cts1-eGFP in the fragmentation zone. Microscopy was performed on agar slides (1% agarose). SG200 expressing cytoplasmic three times $eGFP^3$ was used as a control. Scale bars indicate 5 µm.

Fig. 4 (a-b) Cts1 activity profile of *Ustilago maydis* SG200 and SG200Δumfly1 mutant strains. Cts1 activity from total cell extract **(a)** and cell free culture filtrate (secreted protein extract) **(b)** of *U. maydis* SG200 and SG200Δumfly1 strains were measured by using 4-methylumbelliferyl-β-D-N,N',N''-triacetyl-chitotriose (MUC) as a substrate. The Cts1 activity of the SG200Δumfly1 mutant secreted protein extract is significantly lower than *U. maydis* SG200 strain. There was no significant difference in total cell extract. The *U. maydis* Δ*cts1* mutant was used as a negative control. Significant differences compared to the *U. maydis* SG200 sample are shown with asterisks (** *P*<0,008 and *** *P*<0,0005). For statistical analysis, a one way ANOVA analysis

followed by Dunnett's multiple comparisons test was performed. Error bars represent standard deviation of three biological replicates. **(c-d)** Processing of C-terminally eGFP tagged Cts1-eGFP recombinant protein by *Ustilago maydis* SG200 and SG200Δumfly1 strains. Total proteins were isolated from total cell extract and secreted protein extract of *cts1-eGFP* expressing SG200 and SG200Δumfly1 strains from $YEPS_{light}$ liquid medium (cell density OD_{600}: 1.0). Subsequently, western blot analysis was performed using anti-eGFP antibodies for all samples. In total cell extracts of *U. maydis* SG200 and SG200Δumfly1 strains show only full length Cts1-eGFP protein **(c)**. While the secreted protein extract of SG200Δumfly1 shows only full length Cts1-eGFP protein, *U. maydis* SG200 strain secreted protein extract shows free eGFP, indicating processing of Cts1 **(d)**. The predicted MW of Cts1-eGFP is 82.9 kDa and eGFP is 26 kDa. **(e)** In order to determine the cleavage sites, the cleaved products of Cts1-eGFP after incubation with *U. maydis* culture filtrate were identified via MS/MS analysis. The red arrows labeled bands represent the cleaved products at 46 and 27 kDa. In the schematic diagram, arrows indicate cleavage sites of Cts1-eGFP.

Fig. 5 (a) Microscopic observation of *Ustilago maydis* SG200, SG200Δumfly1, SG200Δumfly1-C, SG200Δumfly1-C_{mut} and SG200Δumfly1-mofly1 complementation strains. Scale bars indicate 20 µm. **(b)** Processing of C-terminally eGFP tagged Cts1-eGFP by *Ustilago maydis* SG200 and mutant strains. Cts1-eGFP was produced and purified by using *Pichia pastoris* protein expression system. An amount of 15 µg of purified ZmChiA were incubated with 30 µl of 50 times concentrated culture filtrates of *U. maydis* SG200, SG200Δumfly1, SG200Δumfly1-C, SG200Δumfly1-mofly1 and SG200Δumfly1-C_{mut} strains, which were isolated from *U. maydis* grown in $YEPS_{light}$ liquid medium (OD_{600}: 1.0). The mixture was then incubated at 28°C for 18 hours. The cleavage of Cts1-eGFP was visualized with western blot analysis using an α-eGFP antibody. Cts1-eGFP incubated with non-inoculated $YEPS_{light}$ (50 times concentrated) was used as a negative control. The predicted MW of Cts1-eGFP is 82.9 kDa and eGFP is 26 kDa. **(c)** Complementation of SG200Δumfly1 mutant with *mofly1* and disease rating. Disease rating of the symptoms caused by the *mofly1* complemented strain (SG200Δumfly1-mofly1) in comparison with SG200, SG200Δumfly1 mutant and SG200Δumfly1-C (UmFly1 complementation) strains at 12 dpi. The SG200Δumfly1-mofly1 only partially restores the virulence on Early Golden Bantam (EGB) maize lines. The infection assay was performed in three independent biological

replicates. A *chi*-squared test was performed to show significant differences (P<0,0001). n= number of infected maize plants. **(d)** Cleavage of N-terminally His and HA tagged ZmChiA recombinant protein by culture filtrate of *Ustilago maydis* SG200, SG200Δumfly1 strains and different complementation strains. The 15 µg of purified ZmChiA was incubated with 30 µl of 50 times concentrated culture filtrate of *U. maydis* SG200, SG200Δumfly1, *umfly1* complementation (SG200Δumfly1-C), *mofly1* complementation (SG200Δ*umfly1-mofly1*) and *UmFly1* active site mutant (SG200Δumfly1-C_{mut}) strains, which was isolated from *U. maydis* grown in $YEPS_{light}$ liquid medium (OD_{600}: 1.0). The mixture was incubated at 28°C for 18 hours. The cleavage of ZmChiA was visualized by Coomassie blue staining of SDS-PAGE. ZmChiA incubated with non-inoculated $YEPS_{light}$ (50 times concentrated) was used as a negative control. The predicted MW of ZmChiA is 32 kDa.

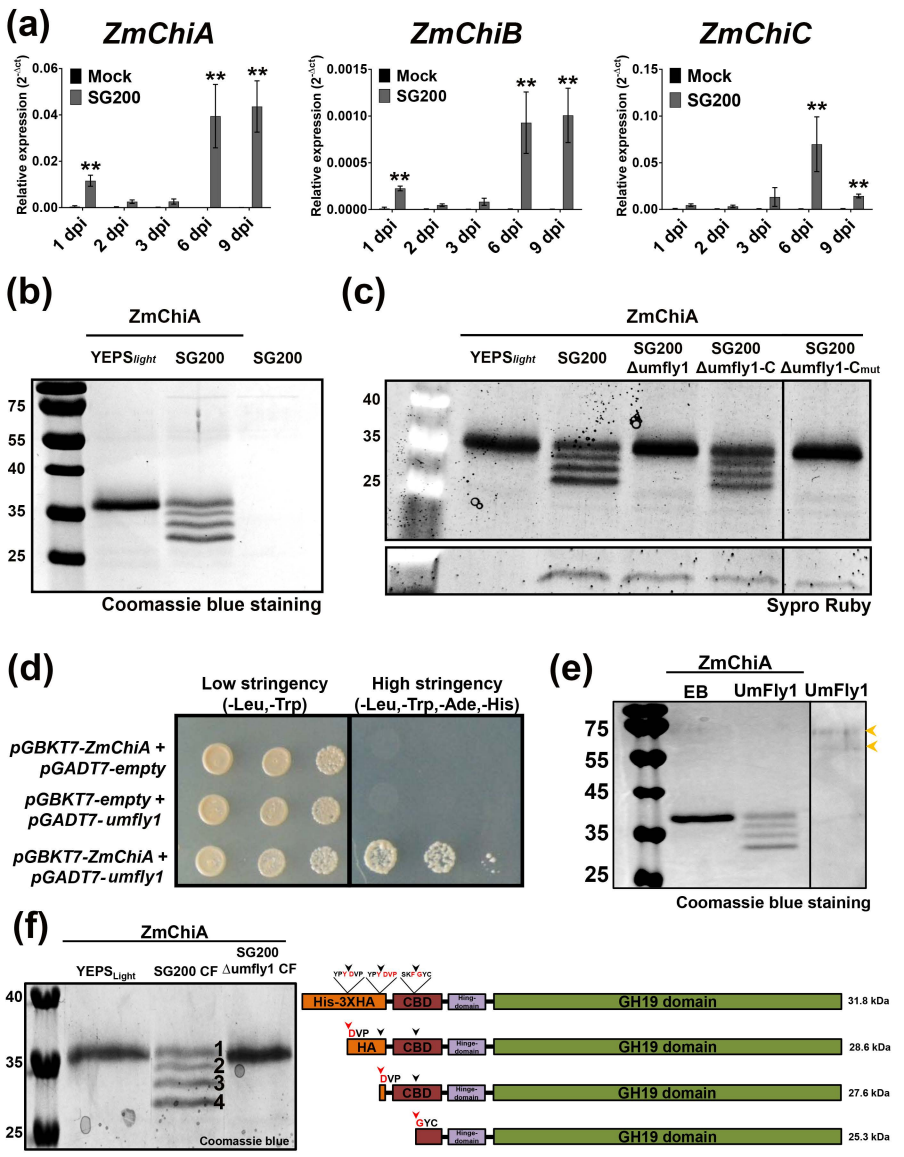
(a)
ZmChiA
ZmChiB
ZmChiC
Relative expression (2-ΔCt)
Mock
SG200
1 dpi
2 dpi
3 dpi
6 dpi
9 dpi
(b)
ZmChiA
YEPSlight
SG200
SG200
Coomassie blue staining
(c)
ZmChiA
YEPSlight
SG200
SG200 Δumfly1
SG200 Δumfly1-C
SG200 Δumfly1-Cmut
Sypro Ruby
(d)
Low stringency (-Leu,-Trp)
High stringency (-Leu,-Trp,-Ade,-His)
pGBKT7-ZmChiA + pGADT7-empty
pGBKT7-empty + pGADT7-umfly1
pGBKT7-ZmChiA + pGADT7-umfly1
(e)
ZmChiA
EB
UmFly1
UmFly1
Coomassie blue staining
(f)
ZmChiA
YEPSLight
SG200 CF
SG200 ΔumflyI CF
Coomassie blue
His-3XHA
CBD
Hinge-domain
GH19 domain
31.8 kDa
28.6 kDa
27.6 kDa
25.3 kDa

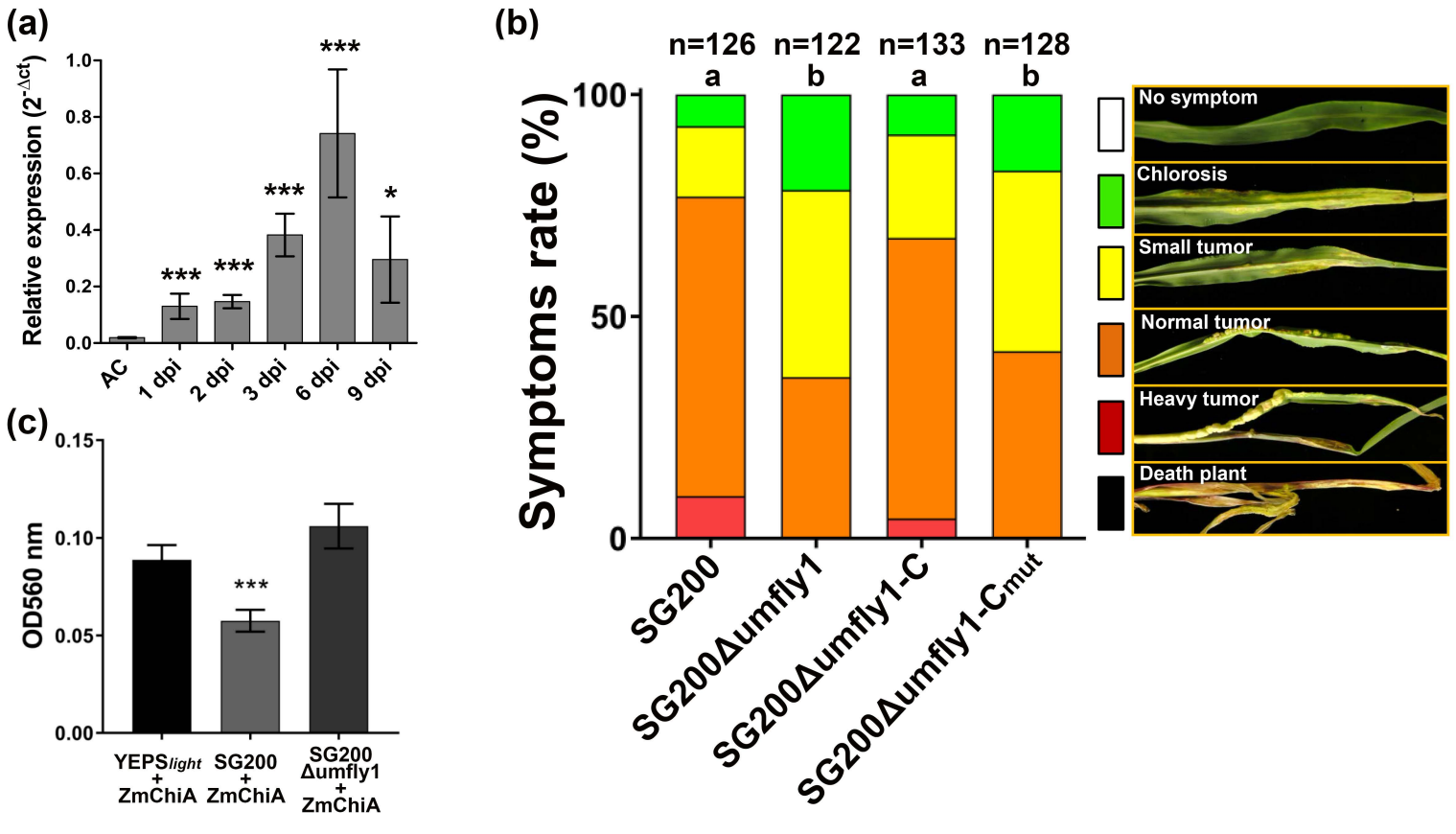
(a)
Relative expression ($2^{-\Delta ct}$)
1.0
0.8
0.6
0.4
0.2
0.0
***
***
***
***
*
AC
1 dpi
2 dpi
3 dpi
6 dpi
9 dpi
(b)
n=126
n=122
n=133
n=128
a
b
a
b
Symptoms rate (%)
100
50
0
SG200
SG200Δumfly1
SG200Δumfly1-C
SG200Δumfly1-Cmut
No symptom
Chlorosis
Small tumor
Normal tumor
Heavy tumor
Death plant
(c)
OD560 nm
0.15
0.10
0.05
0.00
***
YEPSlight + ZmChiA
SG200 + ZmChiA
SG200 Δumfly1 + ZmChiA

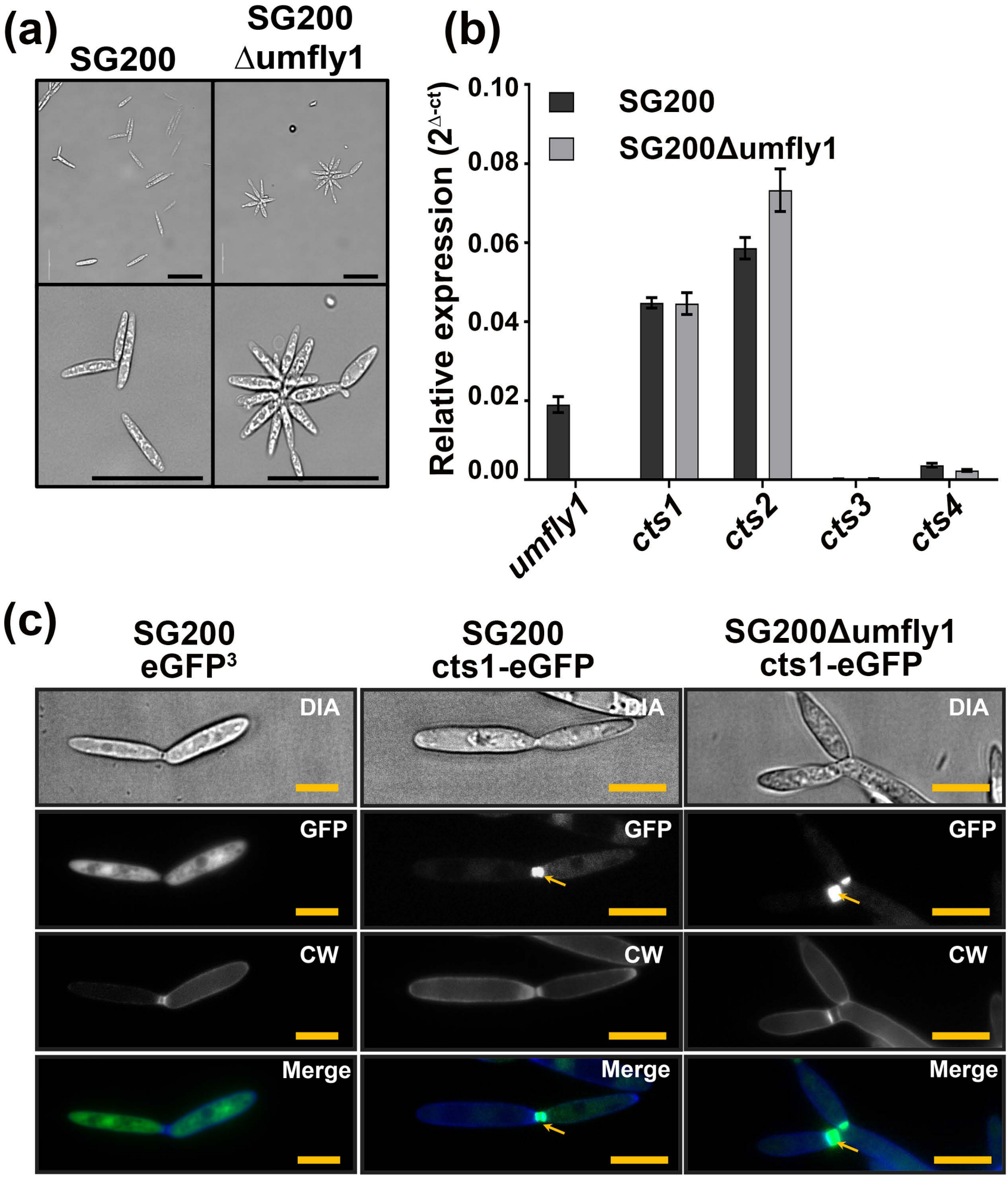
(a)
SG200
SG200 Δumfly1
(b)
Relative expression (2^Δ-ct)
0.10
0.08
0.06
0.04
0.02
0.00
SG200
SG200Δumfly1
umfly1
cts1
cts2
cts3
cts4
(c)
SG200 eGFP3
SG200 cts1-eGFP
SG200Δumfly1 cts1-eGFP
DIA
GFP
CW
Merge

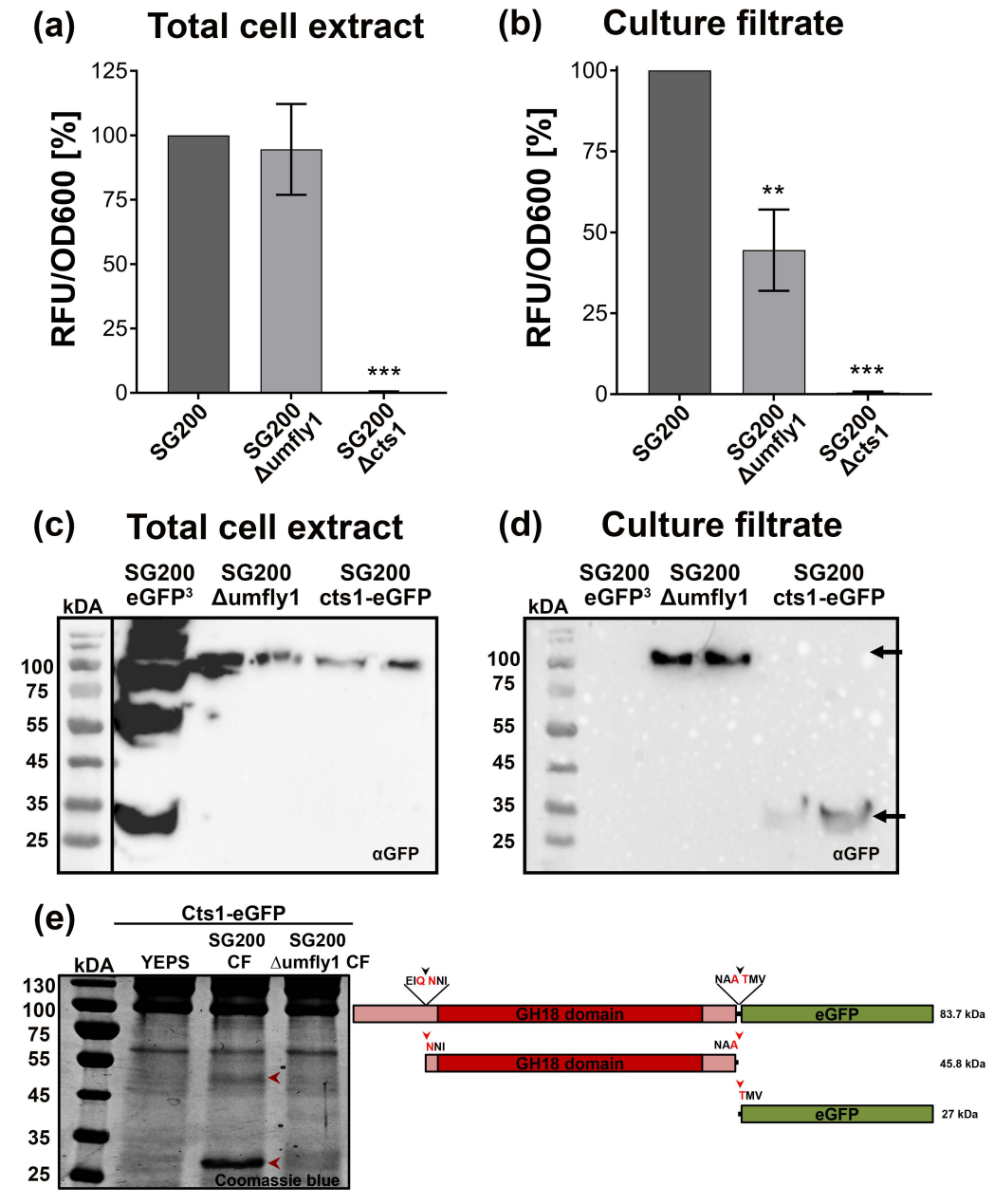
(a)
Total cell extract
RFU/OD600 [%]
125
100
75
50
25
0
***
SG200
SG200 Δumfly1
SG200 Δcts1
(b)
Culture filtrate
RFU/OD600 [%]
100
75
50
25
0
**
***
SG200
SG200 Δumfly1
SG200 Δcts1
(c)
Total cell extract
kDA
SG200 eGFP3
SG200 Δumfly1
SG200 cts1-eGFP
100
75
55
45
35
25
αGFP
(d)
Culture filtrate
kDA
SG200 eGFP3
SG200 Δumfly1
SG200 cts1-eGFP
100
75
55
45
35
25
αGFP
(e)
Cts1-eGFP
kDA
YEPS
SG200 CF
SG200 Δumfly1 CF
130
100
75
55
45
35
25
Coomassie blue
EIQ NNI
NAA TMV
GH18 domain
eGFP
83.7 kDa
NNI
NAA
GH18 domain
45.8 kDa
TMV
eGFP
27 kDa

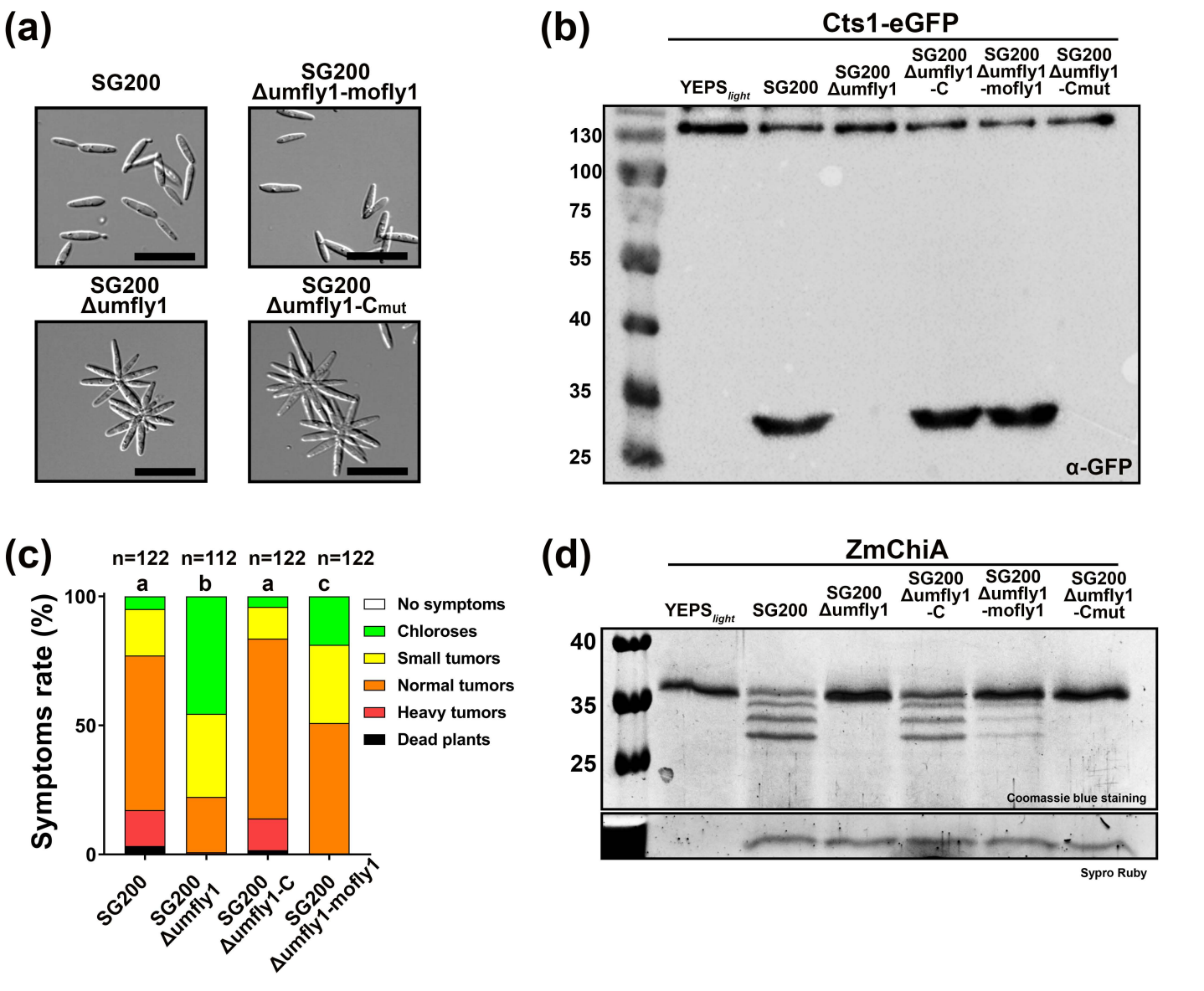
(a)
SG200
SG200 Δumfly1-mofly1
SG200 Δumfly1
SG200 Δumfly1-Cmut
(b)
Cts1-eGFP
YEPS light
SG200
SG200 Δumfly1
SG200 Δumfly1 -C
SG200 Δumfly1 -mofly1
SG200 Δumfly1 -Cmut
130
100
75
55
40
35
25
α-GFP
(c)
n=122
n=112
n=122
n=122
a
b
a
c
Symptoms rate (%)
100
50
0
No symptoms
Chloroses
Small tumors
Normal tumors
Heavy tumors
Dead plants
SG200
SG200 Δumfly1
SG200 Δumfly1-C
SG200 Δumfly1-mofly1
(d)
ZmChiA
YEPS light
SG200
SG200 Δumfly1
SG200 Δumfly1 -C
SG200 Δumfly1 -mofly1
SG200 Δumfly1 -Cmut
40
35
25
Coomassie blue staining
Sypro Ruby